2019-01-0421 Published 02 Apr 2019

Lateral and Tangential Accelerations of Left Turning Vehicles from Naturalistic Observations

Neal Carter, Steven Beier, and Rheana Cordero Kineticorp LLC

Citation: Carter, N., Beier, S., and Cordero, R., "Lateral and Tangential Accelerations of Left Turning Vehicles from Naturalistic Observations," SAE Technical Paper 2019-01-0421, 2019, doi:10.4271/2019-01-0421.

Abstract

When reconstructing collisions involving left turning vehicles at intersections, accident reconstructionists are often required to determine the relative timing and spacing between two vehicles involved in such a collision. This time-space analysis frequently involves determining or prescribing a path and acceleration profile for the left turning vehicle. Although numerous studies have examined the straight-line acceleration of vehicles, only two studies have presented the tangential and lateral acceleration of left turning vehicles. This paper expands on the results of those limited studies and presents a methodology to automatically detect and track vehicles in a video file. The authors made observations of left turning vehicles at three intersections. Each intersection incorporated permissive green turn phases for left turning vehicles. The authors recorded video of left turning vehicles at each intersection from a small unmanned aerial system (sUAS), and that video was analyzed with a convolutional neural network designed to detect vehicles. The detected vehicles were then tracked over time and the results were analyzed. A total of 86 left turning vehicles were analyzed. In 23 of the observed turns, an oncoming vehicle was also visible in the video. The spatial relationship between the oncoming vehicles and the left turning vehicles was analyzed and the relationship between gap acceptance and acceleration is presented. Accident reconstructionists and traffic engineers can use this data to prescribe realistic values or ranges to accelerations of left-turning vehicles.

Introduction

Left turning movements are generally acknowledged to be the highest-risk movements at intersections, and an estimated 27 percent of all intersection-related crashes in the United States are associated with left turns [1]. Although an average of only 10 to 15 percent of traffic turns left at any given intersection, those vehicles are involved in approximately 45 percent of accidents [2].

At signalized intersections, left turning vehicles can be presented with three types of left turn signal phasing: permissive, protected, and protected permissive. Permissive left turn phasing allows left turning vehicles to turn left after yielding to oncoming traffic. For this signal phasing, drivers are presented with a solid green light or a flashing yellow turn arrow. For protected left turn phasing, oncoming traffic is presented with a red signal and left turning drivers are presented with a green turn arrow. In a protected turn phase, left turning drivers are not required to yield to oncoming traffic. Finally, left turning drivers can be presented with both protected and permissive signals consecutively (protected-permissive left turn phasing, or PPLT). Protected left turn phasing has been found to reduce accidents for left turning vehicles, but traffic volume through the intersection is often reduced.

Agent [3] conducted a study in which protected left turn phasing was replaced with permissive left turn phasing at four intersections and found that permissive phasing resulted in a 50 percent reduction in left turn delay, but an increase in left turn accidents. For these intersections, the total number of accidents increased from 44 in the one-year period before the permissive phasing to 78 in the one-year after. The author notes that the only change was the increase in left-turn accidents, and that the frequency of other accidents, such as rear end accidents, did not change.

Fugger, et al. [4] studied accelerations and driver perception-response times for vehicles traveling straight through a signalized intersection. For this study, the authors captured ground level video of two intersections at 120 Hz and analyzed the timing of vehicles crossing the intersections to determine the vehicle accelerations. They found that the acceleration could be modeled with two phases. The initial phase lasted for a mean time of 0.94 seconds, and was characterized by a mean acceleration rate of 0.06 g, while the secondary phase yielded a mean acceleration of 0.22 g.

Happer et al. [5] similarly analyzed video of a signalized intersection to determine vehicle accelerations. In this study, a video camera recorded vehicles passing through the intersection from the 25th floor of an adjacent office building. Happer et al. studied left turning vehicles at the intersection and found that the average turning speed of vehicles that did not stop prior to turning was between 6.0 and 6.6 m/s (13.4 to 14.8 mph), and the average turning speed of vehicles that stopped was between 4.6 and 6.3 m/s (10.3 to 14.1 mph). They also reported that the average acceleration of vehicles that proceeded through the intersection after stopping was between 0.85 and 1.20 m/s^2 (0.087 to 0.122 g). The intersection analyzed by Happer et al. is depicted in Figure 1.

FIGURE 1 Intersection studied by Happer (2009).

Xu et al. [6] analyzed the lateral accelerations of volunteer drivers as they traversed twelve different roadway sections in Sichuan, southwest China. The drivers drove the roadway sections in vehicles that were instrumented to record vehicle accelerations. The authors found that the 50th percentile lateral accelerations for six-lane, four-lane, and two-lane highways were 0.070, 0.096, and 0.167 g, respectively. This study did not include drivers turning left or right, but rather travelling along a roadway that included curved sections.

Muttart [7] studied swerving performances of drivers who were faced with a crash or near crash. In the study Muttart utilized data from 59 swerving events in the InSight (SHRP-2) naturalistic driving study and found that the average lateral acceleration ranged from 0.18 g at three feet of lateral distance travelled and decreased to 0.12 g by the time the drivers travelled laterally more than 12 feet. This study did not present lateral acceleration characteristics for left-turning drivers that were not in crash or near crash events.

The present study seeks to expand on the testing referenced above, and specifically to the Happer, et al. study in several areas. First, the peak lateral accelerations of left turning vehicles are analyzed to determine if lateral acceleration is a more consistent indicator of driver behavior. An added advantage of characterizing turning behavior using lateral acceleration is that the lateral acceleration equation can easily be scaled and applied to intersections of different sizes. This study also expands on the work of Happer et al. by examining the effect of the distance and speed of oncoming vehicles on driver acceleration. Specifically, the correlation between the tangential and lateral accelerations of left turning drivers and the gap that a driver has when they begin their turn is explored.

Data Collection

For this study, three intersections in Denver, Colorado were observed. The intersections did not have protected left turn phasing, so left turning drivers were always required to yield to oncoming vehicles. The first intersection was located at South University Boulevard and Dartmouth Avenue. University Boulevard has a speed limit of 35 mph and has two lanes and a designated turn lane in both the northbound and southbound directions. At the time of the study, there was no protected turning phase. Dartmouth Avenue has a speed limit of 25 mph and has one lane in both the eastbound and westbound directions with a designated left turn lane. There are two northbound and two southbound lanes, and a dedicated left turn lane in each direction. The second intersection studied was Colorado Boulevard and East 35th Avenue. Colorado Boulevard has a speed limit of 40 mph. This is a six-lane road, with three lanes and a designated left turn lane in both the northbound and southbound directions. East 35th Avenue has a speed limit of 30 mph has one lane in both the east and west direction, both without designated left turn lanes. The third intersection was located at South Federal Boulevard and West Kentucky Avenue. Federal Boulevard has a speed limit of 40 mph and has three lanes in the southbound direction and two lanes in the northbound direction. Each direction has a designated left turn lane. West Kentucky Avenue has a speed limit of 25 mph and has one lane in the eastbound and westbound directions, with designated left turn lanes for both. Figures 2, 3, and 4 depict these intersections.

To document traffic in a manner that did not alert drivers that they were being observed, the intersections were observed using a small unmanned aerial system (sUAS, otherwise known as unmanned aerial vehicle - UAV, or drone). All flights were operated in Class G airspace in accordance with the Federal Aviation Administration (FAA) Small Unmanned Aircraft Regulations, Part 107, by a licensed remote pilot. The sUAS was flown above one corner of the intersection at an altitude of 400 ft above ground level and video was taken of

FIGURE 2 Intersection of South University Boulevard and Dartmouth Avenue.

FIGURE 3 Intersection of Colorado Boulevard and East 35th Avenue.

FIGURE 4 Intersection of Federal Boulevard and West Kentucky Avenue.

Map data © 2019 Google.

the traffic patterns. The authors chose to use sUAS footage because it offered advantages over terrestrial camera systems. Namely, the height of the sUAS minimized perspective, and the sUAS could be positioned close to the intersection to collect footage from a perspective that was near perpendicular to the plane of traffic movement.

For the University and Dartmouth intersection, a DJI Phantom 3 Pro sUAS was utilized. This sUAS is equipped with a camera with a 1/2.3" CMOS sensor and a 94° field of view. Video was recorded at 4k resolution (3840 x 2160 pixels) at 29.97 frames per second. For the Colorado Boulevard and East 35th Avenue intersection and the Federal Boulevard and West Kentucky Avenue intersection, a DJI Phantom 4 Pro sUAS was utilized, which is equipped with a camera with a 1" CMOS sensor and an 84° field of view. At these intersections, video was also taken at a 4k resolution (3840 x 2160 pixels) at 29.97 frames per second. For this analysis, all frame rates were assumed to be constant. All videos were taken with the camera in a nadir (straight down) orientation. Once the sUAS was positioned, no control inputs were made, and the GPS system on the sUAS attempted to hold the position.

Data Analysis

Once the footage was captured, clips of left turning vehicles were extracted for analysis. These clips were stabilized in Adobe After Effects [8] to minimize changes in translation, rotation, or scale of the video image resulting from small movements of the drone during recording.

The video clips were then analyzed using YOLO2 (You Only Look Once) [9] algorithm implemented in Keras with a Tensorflow backend, using the "Full Yolo" architecture and "Full Yolo" pretrained weights. YOLO2 is an object detection system that is designed to detect, locate, and identify objects within video frames. The methodology and techniques implemented in the YOLO2 system have been peer-reviewed and published [10,11]. The system first requires the user to train it by labeling objects and object boundaries in training images. To train the system to detect vehicles in aerial footage, the authors used BBox_with_angle-Label-Tool software [12] to label vehicles and vehicle boundaries in 27 frames of footage, with approximately 50 vehicles in each frame. These labeled images were used to train the YOLO2 system to detect vehicles from aerial video. Once training was complete, the trained network was used to detect vehicles in each frame of stabilized sUAS video. The system then exported the bounding box coordinates for each detected vehicle in each frame. Thus, for each frame of video, the trained YOLO2 system detected each vehicle in that frame and exported the coordinates of the geometric center of the bounding box for that vehicle.

However, YOLO2 only detects the objects, and does not recognize one object as being the same or a different object from frame to frame. Each frame is analyzed separately and independent of the other frames. In other words, YOLO2 detects objects, but does not track the movement of individual objects across frames. Houdini software [13] was used in conjunction with the YOLO2 outputs to track the vehicle locations through time and associate the tracked locations with a single vehicle. The detected locations were plotted through time and a path was generated for each vehicle based on the proximity of detected locations in consecutive frames.

This process resulted in an output of a video with labeled bounding boxes, and a text file for each tracked vehicle. The text file contains the pixel coordinates of the center of the bounding box for each frame of the video. Figures 5, 6, and 7 depict this process. Figure 5 is a frame of the video that includes a red vehicle turning left. Figure 6 is that same frame after processing, with labels to indicate the object numbers. In this video, the left turning vehicle is labeled as object 56 and the oncoming vehicle is labeled as object 103. Figure 7 depicts a segment of the text file that results. The first column is the frame of the video, and the second and third columns are the x and y positions of the center of the bounding box, measured in pixels.

The positional data from each left turning vehicle was filtered with a low pass digital Butterworth filter to reduce noise. This filter was a two-channel filter and was run once forwards and once backwards to prevent phase displacements. The filtered positional data was then scaled by measuring the actual distance between discernable objects in the video, such as lane lines and curbs, in Google Earth. The pixel distances in the video were measured using Adobe Photoshop [14] to scale the outputs of the video analysis from pixels to real world units. The use of Google Earth imagery has previously been

FIGURE 5 Video frame before processing.

Map data © 2019 Google.

FIGURE 6 Video frame after processing.

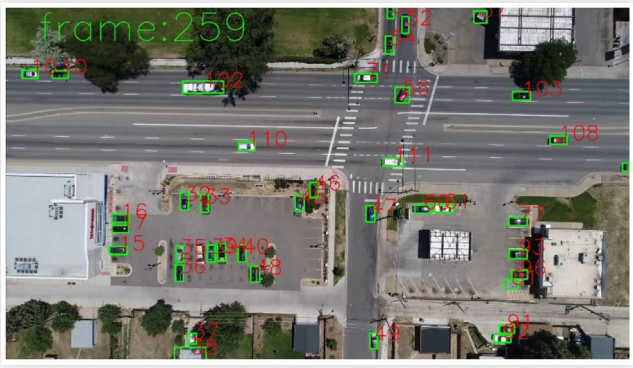

FIGURE 7 Resulting text file from video analysis.

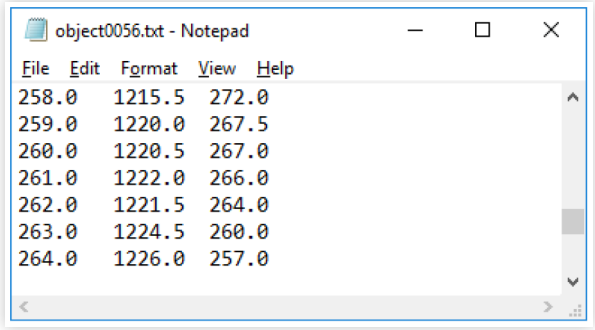

shown to "yield reasonably accurate measurements over the scale of typical accident reconstruction distances" [15]. Once a real-world scale was established, the positional data was utilized to calculate the speed and accelerations of the vehicle as it traversed the roadway.

For this analysis, a time period was selected between when the vehicle first began to enter the oncoming lane(s) to when the vehicle completely cleared the oncoming lane(s). Three representative acceleration values were calculated over this time period. The first value was the average acceleration of the vehicle, calculated as the change in overall vehicle speed over the time that the vehicle was crossing the oncoming lanes. The second calculated value was the peak lateral acceleration. Although the overall vehicle paths were similar to ellipses, the path was modeled as a series of short, constant radius arcs through time to calculate the lateral acceleration. The following equation was used to calculate the path radius:

$$r^2 = (x-h)^2 + (y-k)^2 \quad (1)$$

In this equation, h and k are the coordinates for the center of a circle with a radius, r. The coordinates x and y are on the circle. The video analysis resulted in coordinates for the vehicle center position at each frame. For each left turning vehicle, three points were used to determine the radius of the arc between the three points - the downstream point (x_{i-1}, y_{i-1}), the middle point (x_i,y_i), and the upstream point (x_{i+1},y_{i+1}). The downstream and upstream points were taken at ¼ second before and after the middle point, respectively. The calculated radius was assigned to the middle of the three points. This process involved the following steps:

a. The downstream and middle points for a segment of the video analysis data was entered into the following equation:

$$(x_{i-1}-h)^2 + (y_{i-1}-k)^2 = (x_i-h)^2 + (y_i-k)^2 \quad (2)$$

b. The middle and upstream points were entered into the following equation:

$$(x_i-h)^2 + (y_i-k)^2 = (x_{i+1}-h)^2 + (y_{i+1}-k)^2 \quad (3)$$

c. Equations (2) and (3) represent a system of linear equations with two equations and two unknowns, h and k. Expanding the terms in these equations and rearranging to create linear equations with unknown variables h and k yields Equations (4) and (5).

$$A - B\cdot h - C\cdot k = 0 \quad (4)$$

$$D - E\cdot h - F\cdot k = 0 \quad (5)$$

In Equation (4), the constants A, B, and C are:

$$A = \left[x_{i-1}^2 - x_i^2 + y_{i-1}^2 - y_i^2 \right] \quad (6)$$

$$B = \left[2x_{i-1} - 2x_i \right] \quad (7)$$

$$C = \left[2y_{i-1} - 2y_i \right] \quad (8)$$

In Equation (5), the constants D, E, and F are:

$$D = \left[x_i^2 - x_{i+1}^2 + y_i^2 - y_{i+1}^2 \right] \quad (9)$$

$$E = \left[2x_i - 2x_{i+1} \right] \quad (10)$$

$$F = \left[2y_i - 2y_{i+1} \right] \quad (11)$$

Solving Equations (4) and (5) for the unknown variables, h and k, yields:

$$h = \frac{C\cdot D - F\cdot A}{C\cdot E - F\cdot B} \quad (12)$$

$$k = \frac{A - B\cdot h}{C} \quad (12)$$

d. The radius of the path at the middle point was then calculated with Equation (1). Having calculated the path radius, the lateral acceleration of each turning vehicle was calculated using equation (14), where v is the vehicle velocity and r is the path radius at that point.

$$a_{lat} = \frac{v^2}{r} \quad (14)$$

The third calculated value for each vehicle was the tangential acceleration. This was simply calculated as the change in vehicle speed over two consecutive data points, divided by the time step.

In 23 of the recorded turns, an approaching vehicle in the oncoming lanes was visible in the video frame. In these instances, we calculated the gap in both distance and time to

impact between the left turning vehicle and the oncoming vehicle at the time that the left turning vehicle began to occupy the oncoming lanes. Because the video analysis results in the location of the center of the vehicles, rather than the extents, 11 feet was subtracted from each gap calculation to account for the approximate distance from the center of a vehicle to the front edge (8 feet) plus the approximate distance from the center of a vehicle to the right side (3 feet). The gap time was calculated as the gap distance divided by the speed of the oncoming vehicle as the left turning vehicle began to occupy the oncoming lane(s).

Comparison to VBOX Data

To examine the accuracy of the video analysis method, the authors collected footage for analysis that included an instrumented vehicle driving through the Federal Boulevard and West Kentucky Avenue intersection. The vehicle was equipped with a RaceLogic VB20SL3 VBOX system that continuously measured speed and position at 20 Hz. From the speed and positional data, the VBOX system then calculates lateral acceleration. The VBOX system consisted of an antenna that was affixed to the roof of the vehicle at the approximate longitudinal and lateral center, as shown in Figure 8.

Figures 9 and 10 show the raw data from the VBOX. Figure 9 depicts the vehicle speed through time as the vehicle travelled through the intersection and the surrounding area. Figure 10 depicts the overall vehicle path for the duration of the study, while Figure 11 depicts the path overlaid on an aerial image of the intersection.

The data for each turn was exported and analyzed. A 4-channel phaseless low pass digital Butterworth filter was then applied to the speed, tangential acceleration, and lateral acceleration data reported by the VBOX. A representative comparison of the speed, tangential acceleration, and lateral acceleration is depicted for one of the turns in Figures 12, 13, and 14. In these figures, the data recorded by the VBOX is depicted as a dashed black line, while the solid blue line represents the data that was calculated by analyzing the aerial video. In all, we recorded 10 left turns for comparison.

FIGURE 8 Instrumented vehicle utilized for validation runs.

FIGURE 9 VBOX data, Speed(km/h) vs Time (sec), for all validation studies.

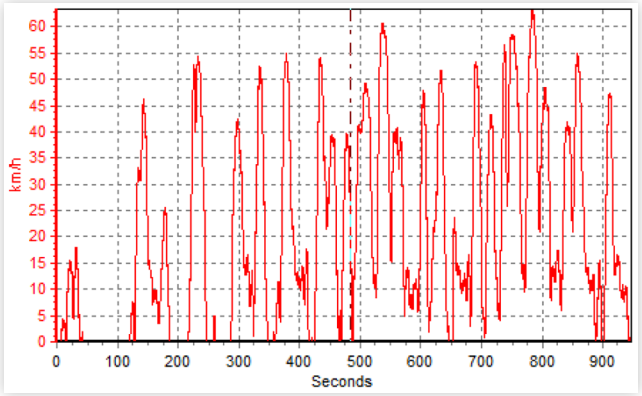

FIGURE 10 Position data from VBOX for all validation studies.

FIGURE 11 VBOX path overlay.

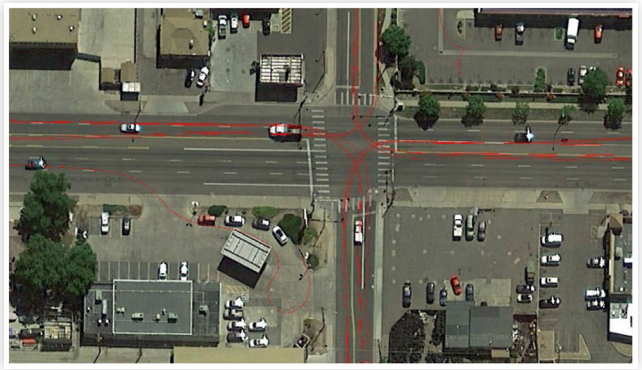

FIGURE 12 Comparison of VBOX measured speed to video analysis speed for one of the instrumented runs.

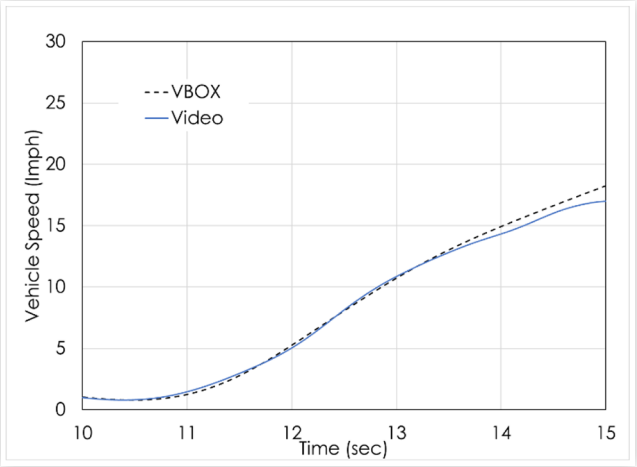

FIGURE 13 Comparison of VBOX measured tangential acceleration to video analysis tangential acceleration for one of the instrumented runs.

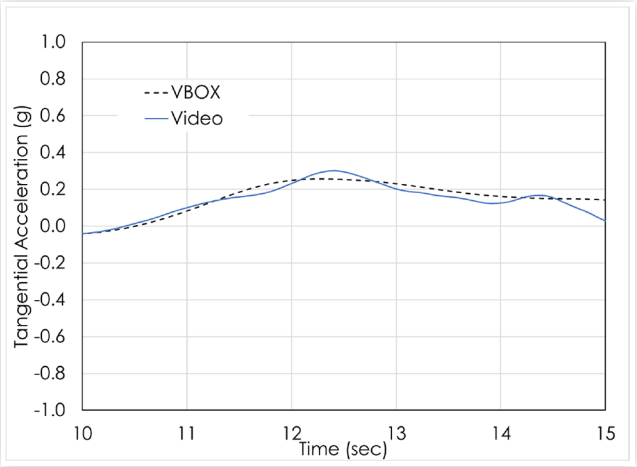

FIGURE 14 Comparison of VBOX measured lateral acceleration to video analysis lateral acceleration for one of the instrumented runs.

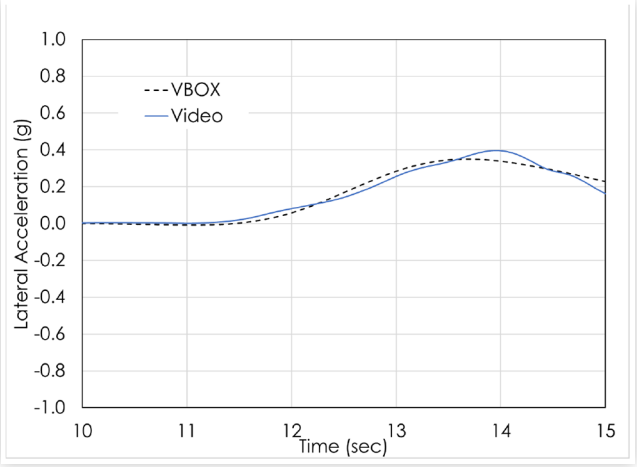

Of interest in the current study is the maximum lateral acceleration, the maximum tangential acceleration, and the average acceleration from the beginning of the left turning vehicle occupying the oncoming lanes to the end of the vehicle occupying oncoming lanes. These values were calculated for each of the instrumented left turns and compared to the VBOX data. The results for each turn are presented in Tables 1, 2, and 3. The video analysis results compared favorably to the VBOX reported values.

Results and Discussion

For each of the 86 left turn vehicles analyzed, the peak lateral acceleration, peak tangential acceleration, and average acceleration was calculated in a manner consistent with the validation left turns described above. In addition, we noted the entry speed, exit speed, and time to traverse the oncoming lanes. The resulting average and standard deviation values are presented in Table 4. Of these left turning vehicles, 86% had a peak tangential acceleration of less than 0.20 g, 81% had a

TABLE 1 Comparison of peak lateral acceleration from vehicle instrumentation and from video analysis.

Turn Number	Peak Lateral Acceleration VBOX (g)	Peak Lateral Acceleration Video Analysis (g)
1	0.39	0.40
2	0.32	0.30
3	0.37	0.38
4	0.35	0.36
5	0.38	0.36
6	0.29	0.28
7	0.35	0.40
8	0.51	0.50
9	0.43	0.40
10	0.36	0.34
Average	**0.375**	**0.372**
Std. Dev.	**0.061**	**0.061**

TABLE 2 Comparison of peak tangential acceleration from vehicle instrumentation and from video analysis .

Turn Number	Peak Tangential Acceleration VBOX (g)	Peak Tangential Acceleration Video Analysis (g)
1	0.21	0.19
2	0.29	0.29
3	0.07	0.14
4	0.18	0.25
5	0.26	0.28
6	0.05	0.07
7	0.24	0.23
8	0.20	0.26
9	0.18	0.19
10	0.16	0.17
Average	**0.184**	**0.207**
Std. Dev.	**0.076**	**0.069**

TABLE 3 Comparison of average acceleration from vehicle instrumentation and from video analysis .

Turn Number	Average Acceleration VBOX (g)	Average Acceleration Video Analysis (g)
1	0.13	0.15
2	0.20	0.20
3	0.03	0.05
4	0.14	0.14
5	0.22	0.22
6	0.04	0.03
7	0.18	0.16
8	0.09	0.09
9	0.15	0.16
10	0.09	0.10
Average	**0.127**	**0.130**
Std. Dev.	**0.064**	**0.062**

TABLE 4 Characteristics of left turning vehicles from entire data set.

All Left Turning Vehicles	Average	Standard Deviation
Entry Speed (mph)	6.38	3.52
Exit Speed (mph)	9.56	4.03
Time to Traverse (sec)	3.25	1.06
Average Acceleration (g)	0.05	0.05
Peak Tangential Acceleration (g)	0.12	0.08
Peak Lateral Acceleration (g)	0.17	0.08

peak lateral acceleration of less than 0.25 g, and 90% had an average acceleration of less than 0.10 g.

For this study, intersections were chosen that required left turning vehicles to traverse one lane, two lanes, or three lanes of oncoming data. Of the 86 left turning vehicles, 28 turned across one lane, 9 turned across two lanes, and the majority (49) turned across 3 lanes. The average values and standard deviation for entry speed, exit speed, time to traverse, average acceleration, peak tangential acceleration, and peak lateral acceleration were analyzed for each number of lanes traversed. These values are presented in Tables 5, 6, and 7.

For left turning vehicles that travelled across one lane, 89% of left turning vehicles had a peak tangential acceleration of less than 0.20 g, 86% had a peak lateral acceleration of less than 0.25 g, and 93% had an average acceleration of less than 0.10 g. For left turning vehicles that travelled across two lanes,

TABLE 5 Characteristics of left turning vehicles transversing one lane.

1 lane Traverse	Average	Standard Deviation
Entry Speed (mph)	6.69	3.93
Exit Speed (mph)	9.74	3.91
Time to Traverse (sec)	3.42	1.35
Average Acceleration (g)	0.04	0.04
Peak Tangential Acceleration (g)	0.10	0.06
Peak Lateral Acceleration (g)	0.18	0.09

TABLE 6 Characteristics of left turning vehicles transversing two lanes.

2 lane Traverse	Average	Standard Deviation
Entry Speed (mph)	9.52	3.27
Exit Speed (mph)	14.09	3.63
Time to Traverse (sec)	2.65	0.34
Average Acceleration (g)	0.08	0.08
Peak Tangential Acceleration (g)	0.23	0.13
Peak Lateral Acceleration (g)	0.29	0.08

TABLE 7 Characteristics of left turning vehicles transversing three lanes.

3 lane Traverse	Average	Standard Deviation
Entry Speed (mph)	5.63	3.00
Exit Speed (mph)	8.63	3.64
Time to Traverse (sec)	3.26	0.93
Average Acceleration (g)	0.04	0.05
Peak Tangential Acceleration (g)	0.10	0.07
Peak Lateral Acceleration (g)	0.15	0.06

33% of left turning vehicles had a peak tangential acceleration of less than 0.20 g, 22% had a peak lateral acceleration of less than 0.25 g, and 67% had an average acceleration of less than 0.10 g. For left turning vehicles that travelled across three lanes, 94% of left turning vehicles had a peak tangential acceleration of less than 0.20 g, 90% had a peak lateral acceleration of less than 0.25 g, and 92% had an average acceleration of less than 0.10 g.

In this study, there were 12 left turning vehicles that were found to have a negative average acceleration. In other words, the entry speed was greater than the exit speed. Of these 12 vehicles, the average and standard deviation for entry speed, exit speed, time to traverse, average acceleration, peak tangential acceleration, and peak lateral acceleration are presented in Table 8.

There was little to no correlation found between the acceleration values that were calculated and the gap that the driver was presented with. Prior to this research, the authors posited that there would be a correlation in these values, such that a shorter gap would be associated with higher accelerations. One possible explanation is that drivers simply chose not to turn through gaps that would require them to accelerate rapidly. This lack of correlation can be seen in Figures 15-20.

TABLE 8 Characteristics of left turning vehicles with a negative average acceleration.

Negative Acceleration	Average	Standard Deviation
Entry Speed (mph)	10.28	4.99
Exit Speed (mph)	8.77	5.33
Time to Traverse (sec)	3.13	0.89
Average Acceleration (g)	-0.02	0.02
Peak Tangential Acceleration (g)	0.07	0.09
Peak Lateral Acceleration (g)	0.19	0.10

FIGURE 15 Peak tangential acceleration vs gap in seconds at entry.

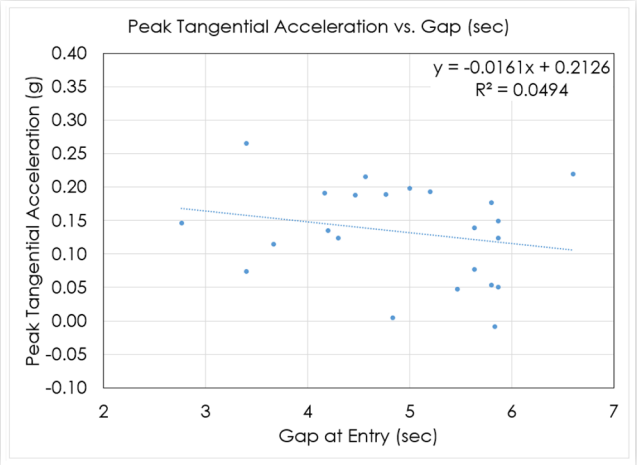

FIGURE 16 Peak lateral acceleration vs gap in seconds at entry.

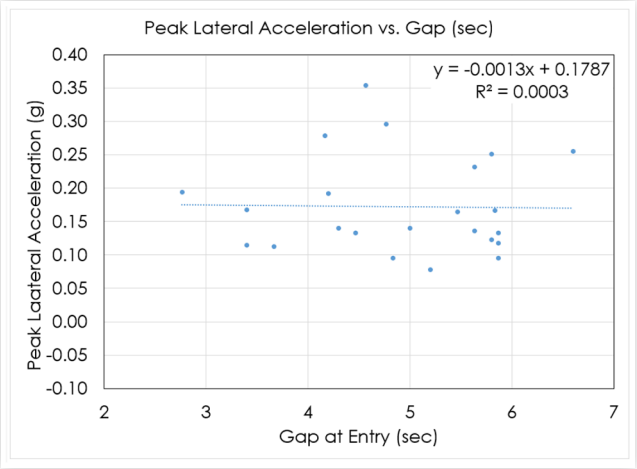

FIGURE 17 Average acceleration vs gap in seconds at entry.

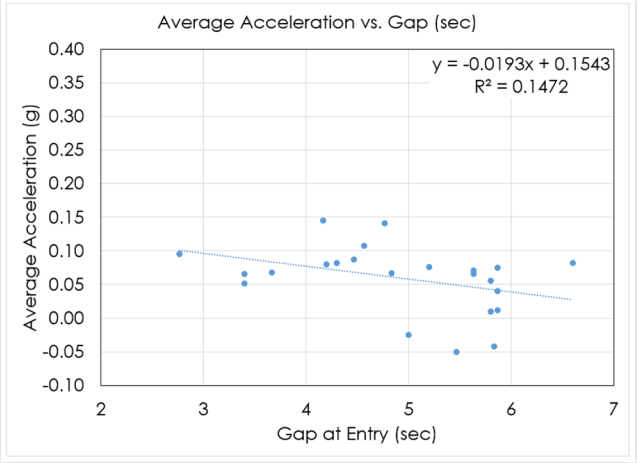

FIGURE 19 Peak lateral acceleration vs gap distance at entry.

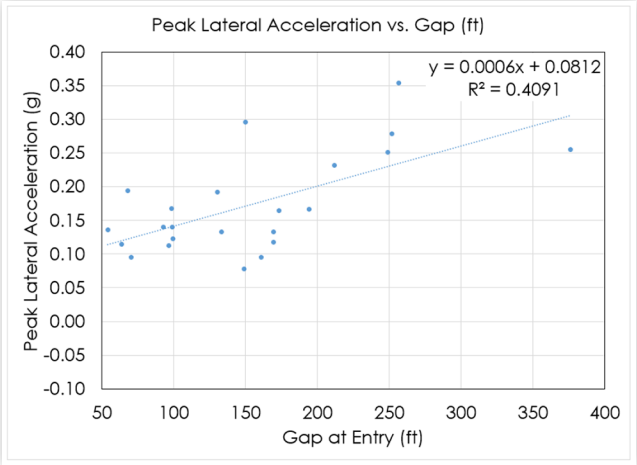

FIGURE 18 Peak tangential acceleration vs gap distance at entry.

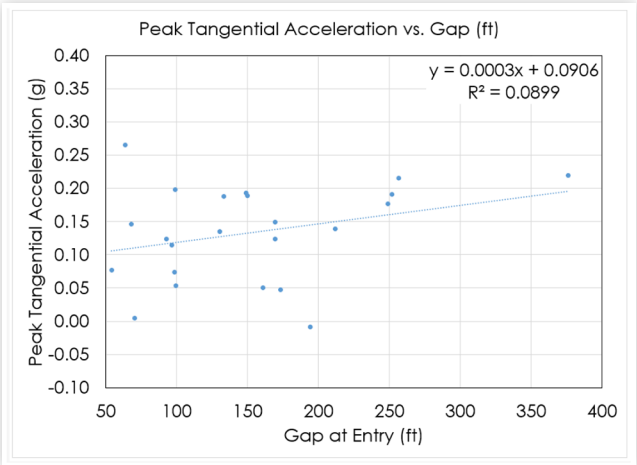

FIGURE 20 Average acceleration vs gap distance at entry.

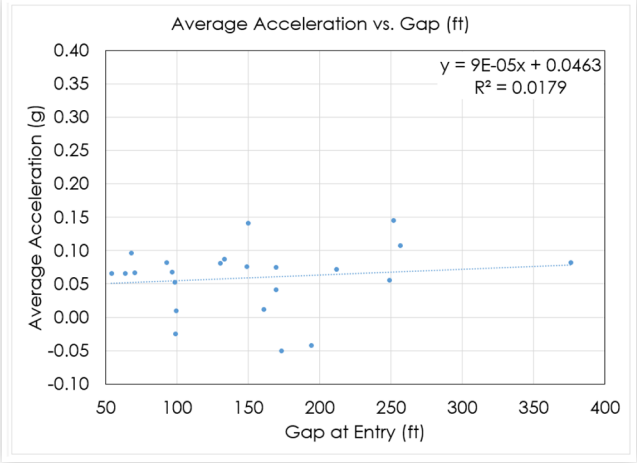

Summary/Conclusions

1. The use of sUAS video footage processed with object detection software is a viable method to determine the speed, lateral acceleration, and tangential acceleration of vehicles through time.
2. In the analysis of 86 left turning vehicles, the average of the peak lateral accelerations was 0.17 g, the average of the peak tangential accelerations was 0.12 g, and the average of the average accelerations was 0.05 g.
3. There was little to no correlation found between the acceleration values that were calculated and the gap that the driver was presented with.
4. Accident reconstructionists and traffic engineers can use the data presented in this paper to prescribe realistic values or ranges to accelerations of left-turning vehicles.

References

1. Permissive/Protected Left Turn Phasing, Federal Highway Administration, U.S. Department of Transportation, FHWA-SA-09-015, https://safety.fhwa.dot.gov/intersection/conventional/signalized/case_studies/fhwasa09015/fhwasa09015.pdf.
2. Maze, T., Henderson, J., and Sankar, R., *Impacts on Safety of Left-Turn Treatment at High Speed Signalized Intersections* (Iowa State University, 1994).
3. Agent, K.R., *An Evaluation of Permissive Left Turn Phasing* (Kentucky Department of Transportation, 1979).
4. Fugger, T., Wobrock, J., Randles, B., Stein, A. et al., "Driver Characteristics at Signal-Controlled Intersections," SAE Technical Paper 2001-01-0045, 2001, doi:10.4271/2001-01-0045.
5. Happer, A., Peck, M., and Hughes, M., "Analysis of Left turning Vehicles at a 4-way Medium-Sized Signalized Intersection," *SAE Int. J. Passeng. Cars - Mech. Syst.* 2(1):359-370, 2009, doi:10.4271/2009-01-0107.
6. Xu, J., Yang, K., Shao, Y., Lu, G., "An experimental study on lateral acceleration of cars in different environments in Sichuan, Southwest China," *Discrete Dynamics in Nature and Society*, 2015, Article ID 494130, 10.1155/2015/494130.
7. Muttart, J., "Influence of Age, Secondary Tasks and Other Factors on Drivers' Swerving Responses before Crash or Near-Crash Events," SAE Technical Paper 2015-01-1417, 2015, doi:10.4271/2015-01-1417.
8. Adobe After Effects (Version 15.0), Computer Software, Adobe, San Jose, CA.
9. Redmon, S., Farhadi, Ali, "YOLO9000: Better, Faster, Stonger", Computer Software, 2016. https://github.com/experiencor/keras-yolo2.
10. Redmon, J., Divvala, S., Girshick, R., Farhadi, A., "You Only Look Once: Unified, Real-Time Object Detection," in *presented at 29th IEEE Conference on Computer Vision and Pattern Recognition (CVPR)*, 2016, https://pjreddie.com/media/files/papers/yolo_1.pdf.
11. Redmon, J., Farhadi, A., "YOLO9000: Better, Faster, Stronger," in *presented at the 30th IEEE Conference on Computer Vision and Pattern Recognition (CVPR)*, 2017, https://pjreddie.com/media/files/papers/YOLO9000.pdf
12. BBox_with_angle-Label-Tool, Computer Software, https://github.com/YenYuHsuan/BBox_with_angle-Label-Tool
13. Houdini (Version 16.5), Computer Software, SideFX, Toronto, Ontario, Canada.
14. Adobe Photoshop CC (Version 19.1.6), Computer Software, Adobe, San Jose, CA.
15. Wirth, J., Bonugli, E., and Freund, M., "Assessment of the Accuracy of Google Earth Imagery for use as a Tool in Accident Reconstruction," SAE Technical Paper 2015-01-1435, 2015, doi:10.4271/2015-01-1435.

Contact Information

Neal Carter
Kineticorp
6070 Greenwood Plaza Blvd, Suite 200
Greenwood Village, CO, 80111
303.733.1888
ncarter@kineticorp.com
www.kineticorp.com

Acknowledgments

The authors wish to thank Connor Smith, for help in acquiring sUAS footage, Nathan Rose, for his helpful review and comments, and the paper reviewers, for their helpful suggestions.

Appendix A- Results Table

Vehicle #	Intersection	Video #	Object #	Initial Travel Direction	# of lanes traversed	Speed at Entry (mph)	Speed at Exit (mph)	Time to Traverse (sec)	Average Accel (g)	Peak Tangential Accel (g)	Peak Lateral Accel (g)	Speed of Oncoming Vehicle (mph)	Gap at Entry (ft)	Gap at Entry (sec)
1	3500-Colorado Blvd	002	75	North	3	4.88	10.13	2.93	0.082	0.11	0.15			
2	3500-Colorado Blvd	002	56	South	3	5.87	8.79	2.53	0.052	0.07	0.17	22.0	99	3.40
3	3500-Colorado Blvd	002	57	South	3	6.35	10.66	2.50	0.078	0.11	0.20			
4	3500-Colorado Blvd	002	58	South	3	6.08	9.20	3.43	0.041	0.12	0.15			
5	3500-Colorado Blvd	003	83	North	3	4.26	8.76	3.00	0.068	0.11	0.11	20.0	97	3.67
6	3500-Colorado Blvd	003	71	South	3	3.99	6.01	3.20	0.029	0.08	0.09			
7	3500-Colorado Blvd	004	107	South	3	1.56	9.49	4.73	0.076	0.19	0.08	21.0	149	5.20
8	3500-Colorado Blvd	004	108	South	3	5.22	9.25	2.27	0.081	0.13	0.19	23.0	131	4.20
9	3500-Colorado Blvd	004	109	South	3	3.61	9.37	3.23	0.081	0.14	0.12			
10	3500-Colorado Blvd	004	98	East	1	5.71	8.59	3.77	0.035	0.11	0.21			
11	3500-Colorado Blvd	004	135	West	1	3.19	3.35	5.53	0.001	0.04	0.04			
12	3500-Colorado Blvd	005	97	North	3	2.64	6.55	2.67	0.067	0.00	0.09	11.5	71	4.83
13	3500-Colorado Blvd	006	73	North	3	9.25	8.90	2.80	-0.006	0.02	0.15			
14	3500-Colorado Blvd	007	66	West	1	4.72	7.16	2.27	0.049	0.06	0.13			
15	3500-Colorado Blvd	009	56	North	3	6.83	7.37	3.73	0.007	0.04	0.10			
16	3500-Colorado Blvd	010	84	West	1	6.57	9.30	3.20	0.039	0.13	0.18			
17	3500-Colorado Blvd	010	54	West	1	8.03	8.75	3.03	0.011	0.04	0.16			
18	3500-Colorado Blvd	011	202	North	3	2.75	10.47	3.50	0.101	0.14	0.13			
19	3500-Colorado Blvd	012	70	West	1	5.85	8.68	5.00	0.026	0.07	0.13			
20	3500-Colorado Blvd	013	71	South	3	4.02	7.12	2.13	0.066	0.27	0.11	15.0	64	3.40
21	3500-Colorado Blvd	014	74	South	3	3.84	2.36	2.73	-0.025	0.20	0.14	15.0	99	5.00
22	3500-Colorado Blvd	014	75	South	3	5.65	8.16	3.10	0.037	0.14	0.20			
23	3500-Colorado Blvd	014	79	South	3	6.75	8.75	3.50	0.026	0.27	0.16			
24	3500-Colorado Blvd	014	78	South	3	7.50	4.94	2.80	-0.042	-0.01	0.17	24.0	194	5.83
25	3500-Colorado Blvd	015	92	West	1	5.30	9.13	3.23	0.054	0.13	0.18			
26	3500-Colorado Blvd	015	43	West	1	8.39	7.79	3.50	-0.008	0.29	0.14			
27	3500-Colorado Blvd	015	27	East	1	7.50	8.47	3.10	0.014	0.09	0.16			
28	3500-Colorado Blvd	015	95	West	1	4.03	8.53	4.13	0.050	0.08	0.14			
29	3500-Colorado Blvd	016	56	South	3	3.47	8.95	3.03	0.082	0.12	0.14	16.5	93	4.30
30	3500-Colorado Blvd	017	150	South	3	7.02	14.77	3.67	0.096	0.15	0.25			
31	3500-Colorado Blvd	017	151	South	3	9.58	13.42	3.13	0.056	0.18	0.25	30.6	249	5.80
32	3500-Colorado Blvd	018	104	West	1	14.43	19.96	2.10	0.120	0.16	0.31			
33	3500-Colorado Blvd	019	92	North	3	14.43	14.08	3.57	-0.004	0.06	0.24			

(*Continued*)

Vehicle #	Intersection	Video #	Object #	Initial Travel Direction	# of lanes traversed	Speed at Entry (mph)	Speed at Exit (mph)	Time to Traverse (sec)	Average Accel (g)	Peak Tangential Accel (g)	Peak Lateral Accel (g)	Speed of Oncoming Vehicle (mph)	Gap at Entry (ft)	Gap at Entry (sec)
34	3500-Colorado Blvd	020	181	South	3	8.07	17.42	2.93	0.145	0.19	0.28	43.0	252	4.17
35	3500-Colorado Blvd	020	184	South	3	10.56	18.33	2.50	0.142	0.19	0.30	23.0	150	4.77
36	3500-Colorado Blvd	020	185	South	3	9.51	18.36	3.30	0.122	0.22	0.27			
37	3500-Colorado Blvd	020	310	East	1	11.53	16.94	3.60	0.068	0.20	0.35			
38	3500-Colorado Blvd	021	122	South	3	2.42	5.70	3.70	0.040	0.06	0.07			
39	3500-Colorado Blvd	021	123	South	3	4.19	6.17	2.50	0.036	0.09	0.12			
40	3500-Colorado Blvd	021	126	South	3	4.29	6.48	2.50	0.040	0.05	0.12			
41	3500-Colorado Blvd	021	130	South	3	6.07	5.92	2.50	-0.003	0.02	0.12			
42	3500-Colorado Blvd	021	127	South	3	5.49	6.33	3.80	0.010	0.05	0.12	13.0	100	5.80
43	3500-Colorado Blvd	021	132	South	3	4.46	5.52	2.20	0.022	0.05	0.09			
44	3500-Colorado Blvd	021	134	South	3	3.78	5.28	2.60	0.026	0.06	0.09			
45	3500-Colorado Blvd	021	172	South	3	4.97	5.68	2.60	0.013	0.04	0.10			
46	3500-Colorado Blvd	021	138	South	3	4.28	1.87	5.40	-0.020	0.03	0.08			
47	3500-Colorado Blvd	022	27	South	3	11.65	15.73	2.60	0.072	0.14	0.23	27.0	212	5.63
48	3100-S University Blvd	001	38	North	2	12.10	13.65	3.00	0.024	0.40	0.32			
49	3100-S University Blvd	003	42	North	2	8.48	13.54	2.80	0.082	0.22	0.26	40.0	376	6.60
50	3100-S University Blvd	004	45	North	2	8.82	18.67	2.10	0.214	0.39	0.38			
51	3100-S University Blvd	004	62	North	2	16.03	13.97	2.90	-0.032	0.05	0.27			
52	3100-S University Blvd	005	53	North	2	8.37	17.93	2.50	0.174	0.31	0.35			
53	3100-S University Blvd	006	65	West	1	20.87	20.76	1.63	-0.003	0.08	0.48			
54	3100-S University Blvd	007	31	North	2	9.88	13.32	2.60	0.060	0.26	0.34			
55	3100-S University Blvd	007	33	North	2	10.87	17.90	2.97	0.108	0.22	0.35	40.0	257	4.57
56	3100-S University Blvd	008	43	East	1	4.80	14.36	2.93	0.148	0.23	0.24			
57	3100-S University Blvd	008	44	East	1	8.78	13.53	3.47	0.062	0.12	0.28			
58	900-S Federal Blvd	001	61	North	3	0.70	8.92	7.00	0.054	0.12	0.15			
59	900-S Federal Blvd	002	81	North	3	3.16	7.81	3.87	0.055	0.09	0.09			
60	900-S Federal Blvd	002	72	North	3	11.35	7.95	3.43	-0.045	0.07	0.18			
61	900-S Federal Blvd	003	62	North	3	3.30	8.26	3.00	0.075	0.15	0.13	21.0	170	5.87

(*Continued*)

© 2019 SAE International. All Rights Reserved.

Vehicle #	Intersection	Video #	Object #	Initial Travel Direction	# of lanes traversed	Speed at Entry (mph)	Speed at Exit (mph)	Time to Traverse (sec)	Average Accel (g)	Peak Tangential Accel (g)	Peak Lateral Accel (g)	Speed of Oncoming Vehicle (mph)	Gap at Entry (ft)	Gap at Entry (sec)
62	900-S Federal Blvd	004	37	North	3	3.83	4.00	2.00	0.004	0.07	0.10			
63	900-S Federal Blvd	005	70	North	3	9.47	8.27	3.17	-0.017	0.03	0.16			
64	900-S Federal Blvd	006	35	North	3	4.84	7.71	3.20	0.041	0.12	0.12	21.0	170	5.87
65	900-S Federal Blvd	007	113	North	3	3.28	9.42	3.20	0.087	0.19	0.13	22.0	133	4.47
66	900-S Federal Blvd	007	117	North	3	1.32	6.67	5.63	0.043	0.08	0.08			
67	900-S Federal Blvd	007	97	North	3	4.82	7.19	3.80	0.028	0.11	0.10			
68	900-S Federal Blvd	008	28	South	2	6.16	8.30	2.83	0.034	0.08	0.15			
69	900-S Federal Blvd	009	45	North	3	3.04	7.57	4.13	0.050	0.07	0.12			
70	900-S Federal Blvd	011	44	North	3	11.84	8.44	3.10	-0.050	0.05	0.16	23.0	173	5.47
71	900-S Federal Blvd	012	33	South	2	5.01	9.57	2.17	0.096	0.15	0.19	19.5	68	2.77
72	900-S Federal Blvd	013	29	North	3	5.28	8.93	2.73	0.061	0.09	0.13			
73	900-S Federal Blvd	014	32	North	3	4.38	5.48	4.23	0.012	0.05	0.10	20.0	161	5.87
74	900-S Federal Blvd	015	35	East	1	6.36	8.38	1.50	0.061	0.09	0.15			
75	900-S Federal Blvd	017	65	East	1	8.75	9.36	2.27	0.012	0.03	0.22			
76	900-S Federal Blvd	018	38	East	1	4.36	7.32	3.83	0.035	0.12	0.14			
77	900-S Federal Blvd	019	36	East	1	7.39	7.75	3.17	0.005	0.03	0.14			
78	900-S Federal Blvd	020	65	East	1	4.42	7.92	4.07	0.039	0.06	0.14			
79	900-S Federal Blvd	020	66	East	1	6.60	9.40	3.63	0.035	0.07	0.18			
80	900-S Federal Blvd	021	30	West	1	4.93	8.51	2.47	0.066	0.08	0.14	7.9	54	5.63
81	900-S Federal Blvd	021	46	East	1	2.06	8.25	3.47	0.081	0.11	0.13			
82	900-S Federal Blvd	021	65	East	1	4.55	5.73	0.70	0.077	0.08	0.06			
83	900-S Federal Blvd	022	48	East	1	4.15	8.66	4.60	0.045	0.09	0.16			
84	900-S Federal Blvd	022	70	East	1	8.34	9.35	2.77	0.017	0.06	0.15			
85	900-S Federal Blvd	023	25	East	1	0.63	8.41	7.33	0.048	0.10	0.14			
86	900-S Federal Blvd	023	26	East	1	5.08	8.33	5.40	0.027	0.07	0.14			
Avg.						**6.38**	**9.56**	**3.25**	**0.047**	**0.12**	**0.17**			
Std. Dev.						**3.52**	**4.03**	**1.06**	**0.047**	**0.08**	**0.08**			
Count						**86**						**23**		

Appendix B- Validation Study Results

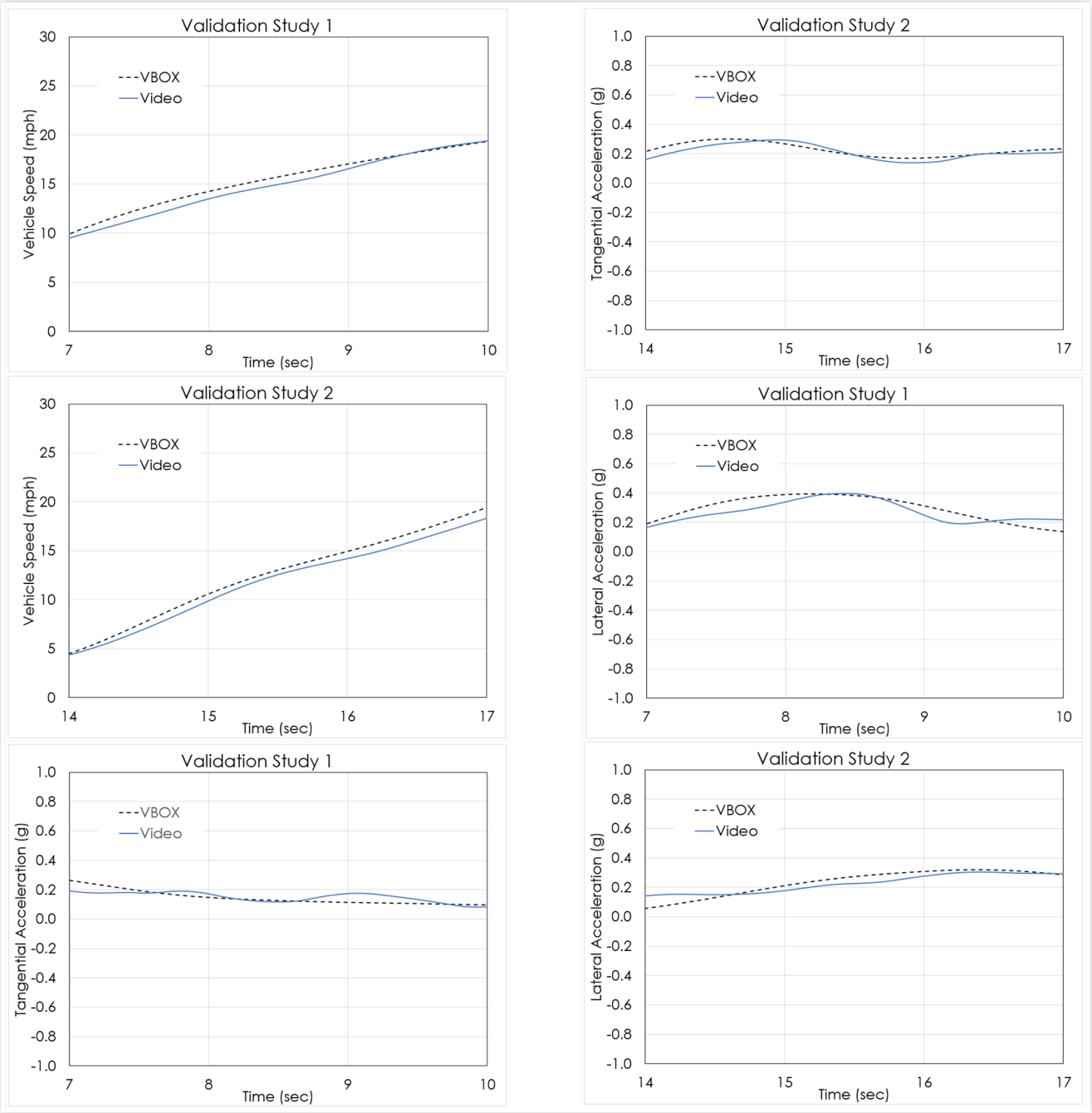

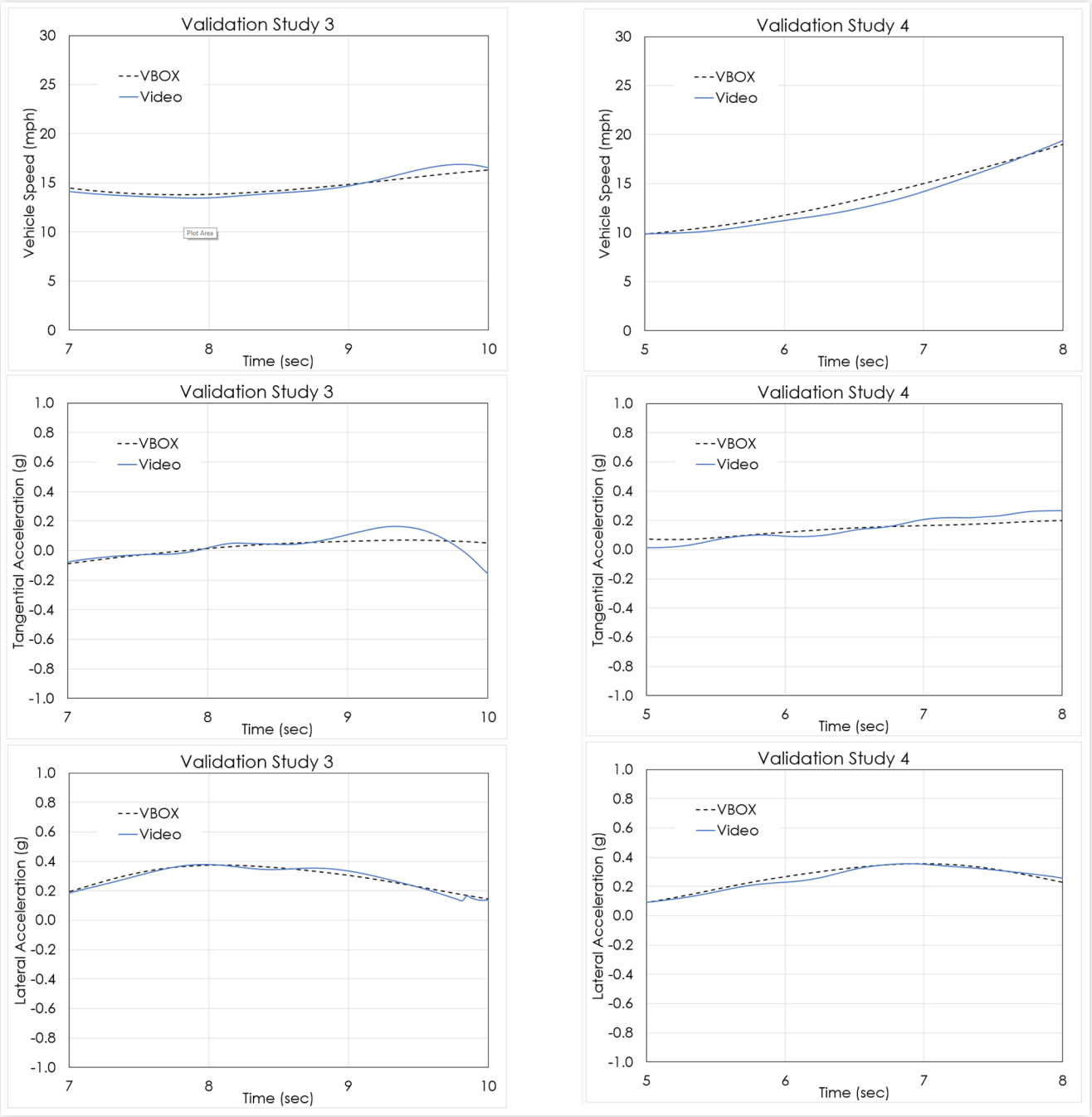

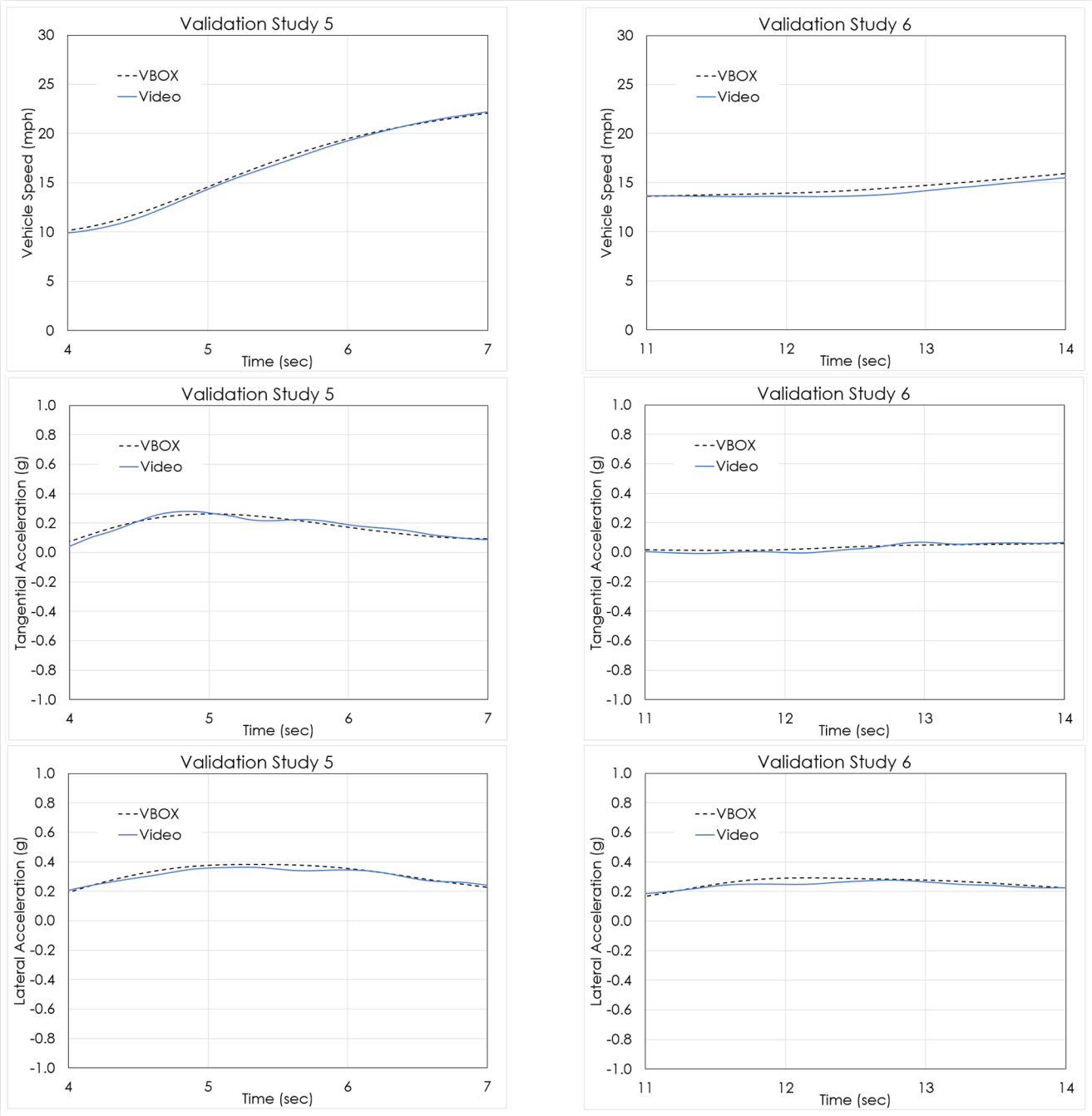

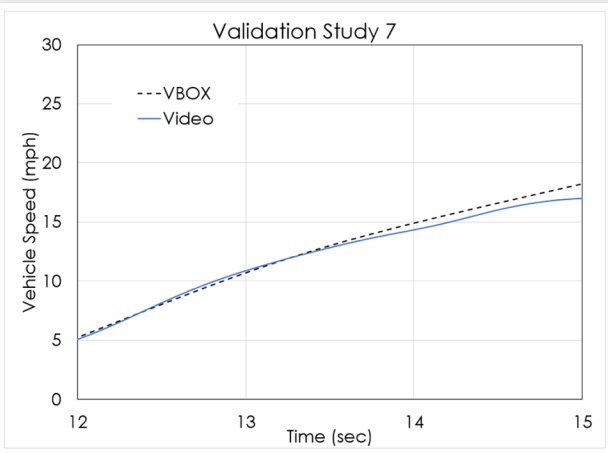

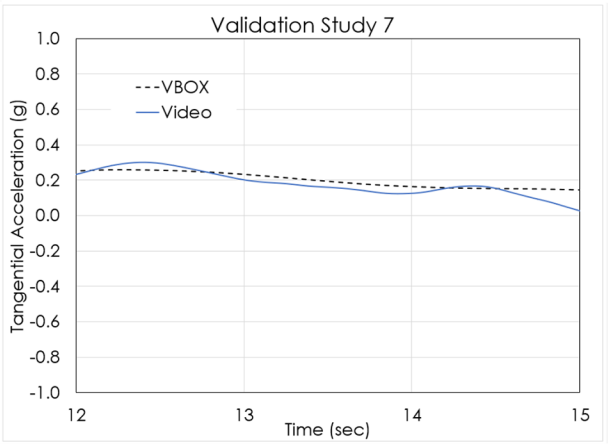

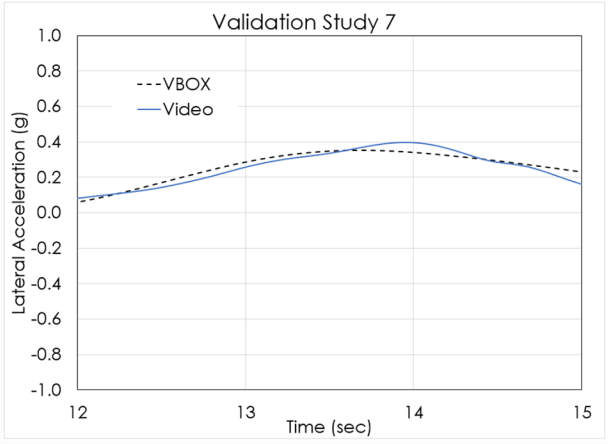

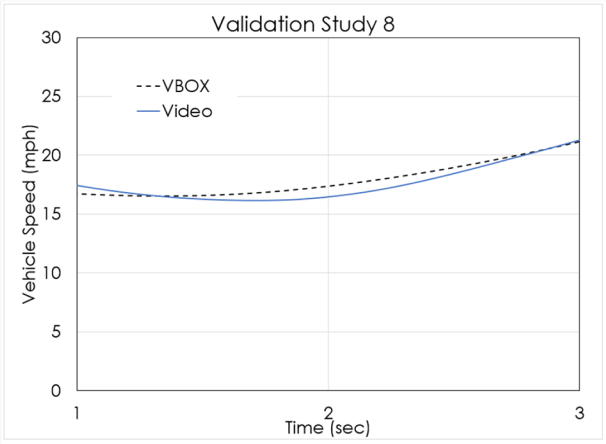

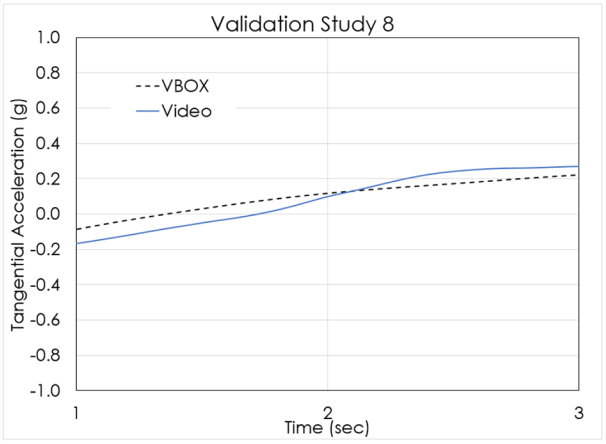

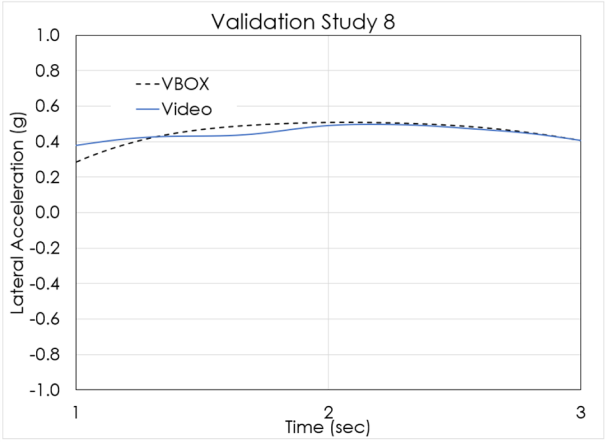

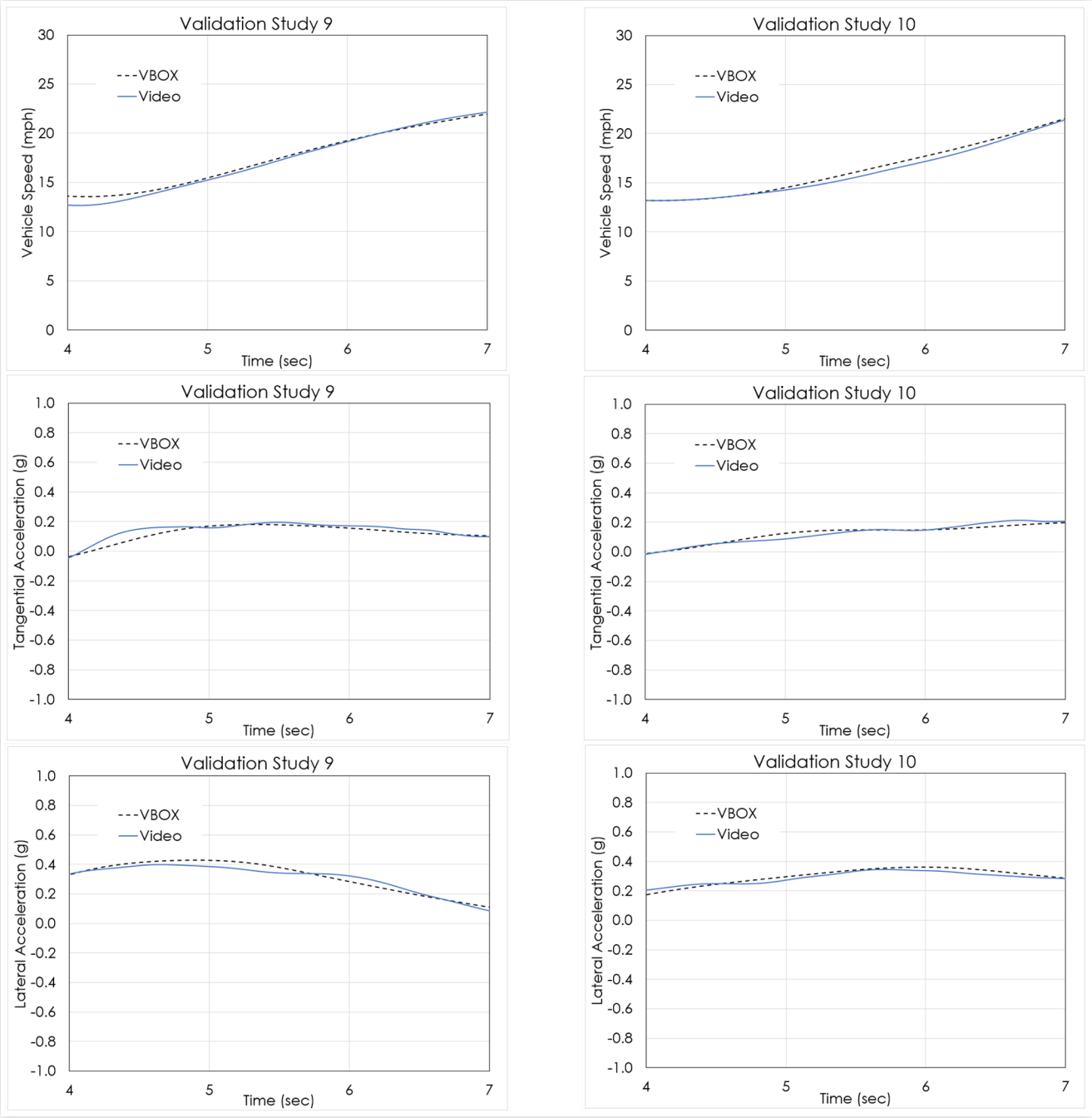

ISSN 0148-7191